A novel mutation in the *daf-19* gene affects ciliated neuron development in *C. elegans*

A Senior Thesis Presented to

The Faculty of the Department of Biology,

The Colorado College

By

Kristen Wells

Bachelors of Arts Degree in Biology

20th day of May, 2013

Dr. Darrell Killian
Primary Thesis Advisor

Dr. Nancy Huang
Secondary Thesis Advisor

Introduction

Cilia and flagella are highly conserved structures that function in movement and sensory reception

Cilia and flagella are highly conserved structures that evolved from specialization of the cytoskeleton (Cavalier-Smith, 2002). Cilia can be either motile or sensory differentiated in part by the microtubule structure: motile cilia consist of a 9 + 2 structure while non-motile (sensory) cilia lack the central microtubule and have a 9 + 0 structure (Reiter et al., 2008, Rosenbaum et al., 2002). One example is the motile cilia found in the paramecium that allow it to move around its environment.

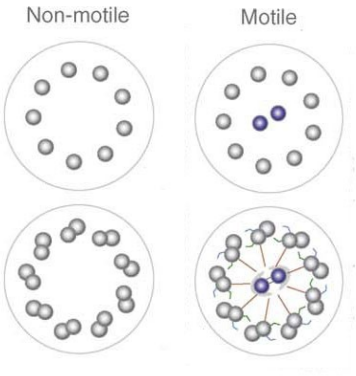

Inglis 2006

Figure 1: non-motile and motile sensory cilia showing the 9+0 structure (left) and the 9+2 structure (right)

The sensory cilia are the cellular antennae that control cell signaling pathways (Satir et al., 2008, Fliegauf et al., 2007). Some examples of sensory cilia in humans are found in the retina, the inner ear, and the nasal epithelium (Rosenbaum et al., 2002, Fliegauf et al., 2007). The sensory cilia of the eye in the retina are photoreceptors that detect light intensities and wavelengths (Ibañez-Tallon et al., 2003, Fliegauf et al., 2007). Inner ear sensory cilia are necessary for both hearing and balance (Fliegauf et al., 2007). In the inner ear, auditory vibrations are converted

into electrical signals (Fliegauf et al., 2007). The sensory cilia of the nasal epithelium are chemoreceptors and detect oderant molecules from the environment (Fliegauf et al., 2007).

Defects in mammal sensory cilia lead to polycystic kidney disease, retinitis pigmentosa, and Bardet-Biedl syndrome (Satir et al., 2008, Filegauf et al., 2007). Polycystic kidney disease leads to kidney failure (Singla et al., 2006). Normal kidney function relies on bending of primary cilia within the kidney in response to urine flow (Singla et al., 2006). The bending of the cilia causes an increase in Ca^{2+} and causes a signal cascade that deactivates cell proliferation and cyst development (Singla et al., 2006). Defects to sensory cilia causes a no flow response even in the presence of urine (Singla et al., 2006). A better understanding of the assembly of sensory cilia and their specification for different sensory signaling pathways will ultimately lead to therapies for cilia diseases through the development of genetic tests.

Transcription factors control the development of cilia

The development of sensory neurons is in part controlled by transcription factors (Chung et al., 2012). Transcription factors must bind to specific cis-regulatory sequences within the DNA in order to promote transcription of key target genes and therefore are important in gene regulation (Tuch et al., 2008). An important family of transcription factors in the development of cells with sensory cilia are the RFX transcription factors (Reith et al., 1990, Reith et al., 1994, Bonnafe et al., 2004, Chung et al., 2012, Burghoorn et al., 2012). These transcription factors bind to X box sequences of DNA and promote transcription (Reith et al., 1990). The RFX transcription factors have a DNA-binding and dimerization domain and show strong homology within eukaryotic cells therefore binding to similar or identical X box sites (Reith et al., 1990). Seven distinct RFX genes have been identified in mammals based on a highly conserved DNA

binding domain (Aftab et al., 2008, Emery et al., 1996). The RFX transcription factors have been found to play a large role in ciliogenesis (Reith et al., 1990, Reith et al., 1994, Bonnafe et al., 2004, Chung et al., 2012, Burghoorn et al., 2012). The RFX3 transcription factor is involved in cilia formation and targets *D2lic* in mammals, a gene encoding a protein involved in cilia formation (Bonnafe et al., 2004). RFX2 is also essential for ciliogenesis in mammals although it does not affect specification of cilia (Chung et al., 2012).

Since mammals have seven different RFX transcription factors and numerous cell types with sensory cilia, the study of ciliogenesis in mammals is difficult. The model organism *Caenorhabditis elegans*, a soil nematode has emerged as an excellent subject for the study of ciliogenesis because it contains a single RFX transcription factor and has a small number of cells with sensory cilia, which can be directly observed in living animals. The lone *C. elegans* RFX transcription factor is called DAF-19 and alignments with mammalian RFX transcription factors showed DAF-19 to have a highly conserved DNA binding domain (Swoboda et al., 2000). Similarly to mammalian RFX transcription factors, DAF-19 is a transcriptional activator of genes involved in cilia development (Swoboda et al., 2000). *daf-19* functions in the formation of ciliated neurons as well as the specification of these neurons (Swoboda et al., 2000). The *daf-19(m89)* homozygous null mutant males completely lack ciliated neurons such as CEM head neurons and HOB and RnB tail neurons (Swoboda et al., 2000). The *daf-19(m89)* homozygous null animals also express the dauer phenotype: they are smaller and never reach reproductive maturity (Swoboda et al., 2000). DAF-19 has four isoforms: DAF-19A, DAF-19B, DAF-19C, and DAF-19M (see figure 2) (Swoboda et al., 2008, Wang et al., 2010).

DAF-19A/B are expressed in nonciliated neurons and play a role in the control of synaptic vesicle proteins although these isoforms do not regulate synaptic genes at the

transcription level (Senti et al., 2008). DAF-19C is only expressed in ciliated neurons and targets cilia-promoting genes directly via the x-box and transcriptional regulation (Senti et al., 2008).

The DAF-19M isoform is required for the cilia specialization of male-specific cells that express several genes that all function together in a subset of ciliated neurons (known as PKD neurons) but is not required for dauer formation, ciliogenesis, or expression of ciliogenic genes (Wang et al., 2010). This isoform activates the PKD gene battery and is expressed in the mail tail HOB and RnB neurons as well as the CEM head neurons (Wang et al., 2010). While the HOB and RnB neurons do not develop until the fourth larval stage, CEM neurons are born during embryogenesis but the CEM neurons do not express *daf-19m* until late L4 (Wang et al., 2010).

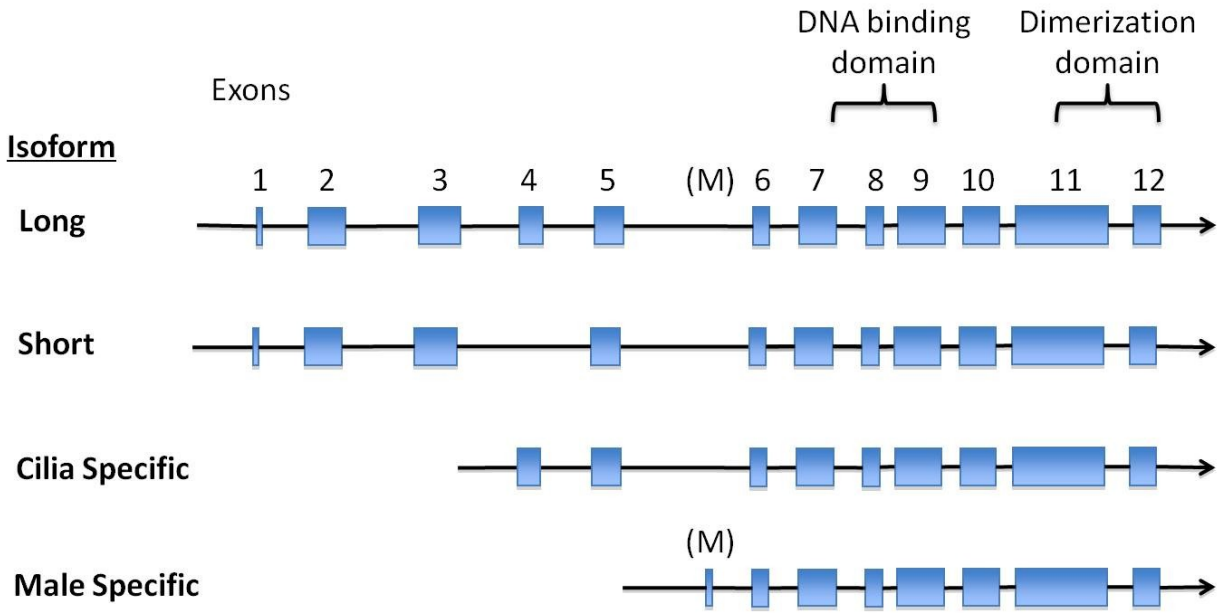

Figure 2: Four isoforms of *daf-19*. Long (DAF-19A), short (DAF-19B), cilia specific (DAF-19 C), and male specific (DAF-19 M)

Although the four isoforms of DAF-19 are important for sensory cilia development, it acts late in the cascade of events for neuron development; therefore it does not affect cell fate, but instead impacts specific function in ciliated sensory neuron differentiation (Swoboda et al., 2000). Because of the importance of DAF-19 in ciliogenesis, a *daf-19* null mutant will not

express PKD::GFP in the CEM, RnB, or HOB neurons of the male and will be dauer (Swoboda et al., 2000). The dauer stage is an alternative larval stage that can endure harsh environmental conditions (Swoboda et al., 2000). When conditions improve, the dauer larva can recover and resume normal development, but this recovery is dependent upon amphid sensory neurons and therefore does not occur in *daf-19 (m89)* null mutants (Swoboda et al., 2000).

The transcription factor DAF-19 controls the development of sensory cilia in C. elegans

Sensory cilia are assembled through the process of interflagellar transport (IFT) (Rosenbaum et al., 2002). During IFT, proteins are moved to the distal tip of the cilia by motor proteins called kinesins and dyneins that move along the microtubule (Rosenbaum et al., 2002, Hirokawa 1998). Two separate kinesin motors, Osm-3-kinesin and kinesin-II, build sensory cilia on *C. elegans* neurons (Snow et al., 2004). These two motors are used to build the sensory cilia in *C. elegans* that make up 60 of 302 total neurons (Inglis et al., 2006). Some of these ciliated neurons are required for chemoreception and mechanoreception required to locate the hermaphrodite vulva (Chasnov et al., 2007, Bae et al., 2008, Liu et al., 1995, Simon et al., 2002). In mammals, including humans, kinesin motors are required to build the sensory cilia in the retina, ear, and kidney (Filegauf 2007).

DAF-19 targets many genes required for ciliogenesis. One recently identified gene targeted by DAF-19 is *xbx-1*, a gene involved in IFT and a homolog to *D2lic* in mammals (Schafer 2003, Bonnafe et al., 2004). DAF-19 is also required for *pkd-2*, *lov-1*, and *klp-6* expression, but the actual mechanism of transcriptional regulation is unknown; these genes do not appear to have an X box in their regulatory regions (Peden et al., 2005). *lov-1* and *pkd-2* function in the same pathway for functional specification of male specific ciliated neurons, but

they do not act in the earlier ciliogenesis step (Peden et al., 2005, Barr et al., 2001). They are expressed in the CEM, RnB, and HOB neurons and are required for male mating behaviors, response, and vulva location (Barr et al., 2001). Together *lov-1* and *pkd-2* form a ion channel in the neuron that facilitates movement of ions in order to cause an action potential (Barr et al., 2001).

lov-1 and *pkd-2* are homologs of the human genes PKD1 and PKD2 which code for polycystein-1 and polycystein-2, two transmembrane proteins essential in the ciliated neurons of the kidney (Barr et al., 1999, Singla et al., 2006). In *C. elegans*, *pkd-2* and *lov-1* are likely transported by the IFT protein *klp-6* (Peden et al., 2005). DAF-19 is also directly involved in the regulation of IFT proteins such as *osm-6*, *che-2*, and *osm-1* (Swoboda et al., 2000). These IFT proteins are responsible for the physical building of the ciliated neurons (Hirokawa 1998).

DAF-19 is involved in the ciliogenesis of male specific ciliated neurons (Swoboda et al., 2000). These neurons include the CEM in the head and the RnB and HOB neurons in the tail (wormatlas.org). The CEM neurons in the head are involved in chemoreception and can detect pheromones involved in sexual attraction from the hermaphrodite (wormatlas.org). Defects in CEM neurons prevent male *C. elegans* from chemosensing the hermaphrodite and therefore mating. The RnB and HOB neurons are located in the tail of the male and are involved in mechanoreception (wormatlas.org). The HOB neuron is part of the hook of the male tail and is required for sensing the hermaphrodite vulva during mating (wormatlas.org). The RnB neurons are ray neurons that innervate the male tail (wormatlas.org). Like the HOB neuron, the RnB neurons are important in sensing the hermaphrodite vulva during mating (wormatlas.org).

During mating, the *C. elegans* male must first locate the hermaphrodite (reviewed by Hartwell et al., 2008). Once this happens, the male lies next to the hermaphrodite and slides the

fan-shaped tail along the hermaphrodite until it locates the vulva (reviewed by Hartwell et al., 2008). The male then inserts specialized structures in the tail into the vulva and ejaculates the sperm that will fertilize the eggs (reviewed by Hartwell et al., 2008).

Here we report the isolation and characterization of *daf-19(sm129)* a point mutation in the *daf-19* gene. We show that the *daf-19(sm129)* mutant males have no *pkd-2* expression in CEM neurons and reduced expression in HOB and RnB neurons as assayed by *pkd-2::GFP*. Although the point mutation affects splicing, incorrect splicing occurs only a portion of the time and some correctly spliced products are formed as assayed by reverse transcriptase PCR. From this study we can conclude that *daf-19* isoforms are needed at different levels of expression and only a small amount of *daf-19* is needed for cilia formation and dauer pathway regulation whereas a much higher level of *daf-19* expression is needed for the functional specification of PKD neurons such as CEMs, HOBs, and RnBs.

Methods

Strains and culture methods

smIs26[pkd-2::GFP]; daf-19(sm129)/mIn1(mIs14); him-5(e1490)

smIs26[pkd-2::GFP]; unc-4(e120) bli-1(e769)

smIs26[pkd-2::GFP]; daf-19 (sm129); him-5(e1490)

smIs23[pkd-2::GFP]; daf-19 (sm129); him-5(e1490)

him-5(e1490)(e1490)

smIs26[pkd-2::GFP]; daf-19(m86)

dhIs59: Expressed in a ventral pair of bilateral neurons identified as the IL1Vs or URAVs in the anterior ganglia; perinuclear. By mid-L2, expression in the cytoplasm of the

hypodermis, the syncitial epidermis, but absent from midline, epidermal seam cells. Levels peak around the L2 molt and diminish during L4. In some cases, transient expression seen in the L3 vulval blast cells. Also expressed within the hermaphrodite spermatheca starting in late L4 larvae and continuing eve in old adults. In males, expression is in IL1V/URAVs and hypodermis but not in the somatic gonad. In dauer larvae, strong expression in IL1V/URAv and specifically extends into axonal but not dendritic processes. In post-dauer stages, expression in a pattern similar to reproductively growing animals, except expression is absent in the hypodermis. Grow at 20C. May still contain lin-15(n765) mutation in the background.

ynIs80[Pflp-21::GFP] and *ynIs87[Pflp-21::GFP]*: flp-21 encodes a single FMRFamide-related neuropeptide (FaRP) that serves as a ligand for NPR-1, a G protein-coupled receptor that regulates social versus solitary feeding behavior in several *Caenorhabditis* species; genetic analysis suggests that FLP-21 acts through NPR-1 to inhibit social feeding behavior; FLP-21 is expressed in the ADL, ASE and ASH sensory neurons, the URA motor neurons, the MC, M2 and M4 pharyngeal neurons, and the intestine; flp-21 encodes the only FMRFamide-related neuropeptide (FaRP) encoded by the *C. elegans* genome that activates both the social (215F) and the solitary (215V) forms of NPR-1 in both Xenopus oocytes and pharyngeal assays.

lin-15B(n765) X; akEx32: lin-15B encodes a novel protein that contains a THAP domain, a zinc-coordinating, site-specific DNA-binding domain; lin-15B was first identified as a class B synMuv gene that acts redundantly with lin-15A to negatively regulate the outcome of Ras signaling during vulval cell fate specification; subsequently, lin-15B has

been shown to also negatively regulate progression through the G1 phase of the cell cycle and RNA-mediated interference (RNAi).

Des2::GFP(hmIs4): des-2 encodes an alpha subunit of nicotinic acetylcholine receptor (nAChR), predicted to be a ligand-gated ion channel regulating the fast action of acetylcholine at neuromuscular junctions and in the nervous system; DES-2 is coexpressed with and genetically interacts with DEG-3, which which it probably forms heteromultimers, and DES-2 falls into the 'DEG-3' class of nAChR subunits, probably unique to nematodes, which includes DEG-3, ACR-5, ACR-17, ACR-18 ACR-20, and ACR-23.

osm-6::GFP: *osm-6* encodes a novel protein that is orthologous to the IFT52 component of the intraflagellar transport particle; osm-6 activity is required cell autonomously for proper sensory cilium structure and thus for normal ciliated sensory neuron function; OSM-6 is a component of the intraflagellar transport particle subcomplex B, and OSM-6::GFP reporter fusions are expressed exclusively in ciliated sensory neurons. daf-19 (sm129)/mIn1(mIs14); smIs26[pkd-2::GFP]; him-5(e1490) male C. elegans were crossed with hermaphrodites expressing osm-6::GFP to make a daf-19 (sm129); osm-6::GFP; him-5(e1490) strain.

smIs26[pkd-2::GFP]; rrf3(pk1426); him-5(e1490)(e1490)

rrf-3(pk1426)

All worms were grown at 20C except for crosses with *smIs26; daf-19(m86)* mutants which were grown at 15C.

Mapping daf-19 (sm129) to a chromosome

The *daf-19 (sm129)* was mapped to LG II using the *mIn1(mIs14)* LG II balancer chromosome. Animals heterozygous for *daf-19 (sm129)* and also heterozygous for the *mIn1(mIs14)* balancer chromosome were allowed to self-fertilize and 100% of the animals with the *daf-19 (sm129)* CEM phenotype were not carriers of the *mIn1(mIs14)* chromosome.

Deficiency mapping

Complementation tests were done between *smIs26[pkd-2::GFP]; daf-19 (sm129); him-5(e1490)* mutants hermaphrodites heterozygous for deficiencies on LG II. The F_1 progeny were scored for number of CEM neurons in the male. If an average of four neurons were found, the wild type phenotype was observed, if an average of less than two neurons were found, the *daf-19 (sm129)* phenotype was assumed to be observed. Based on the presence of the *daf-19 (sm129)* phenotype, a rough estimate of the gene location was made.

3-Factor Mapping

unc-4(e120) and *bli-1(e769)* were used as markers with which to map the location of *daf-19 (sm129)*. *unc-4(e120)* is at map position LG II: 1.77 cM. *bli-1(e769)* is at map position CHII: 3.12 cM. A *smIs26[pkd-2::GFP]; unc-4(e120) bli-1(e769)* strain was made. *smIs26[pkd-2::GFP]; unc-4(e120) bli-1(e769)* hermaphrodites were crossed with *smIs26[pkd-2::GFP]; daf-19 (sm129)/mIn1(mIs14); him-5(e1490)* males. Unc non-Bli and Bli non-Unc animals were picked for in the F_1 generation. A fluorescence microscope was used to observe the males for *daf-19 (sm129)* phenotype by counting CEM neurons in the head of the worm. The number of cross over events between *bli-1(e769)* and *unc-4(e120)* that segregated the CEM phenotype was

used to determine the relative map position of the *daf-19 (sm129)* mutation. This experiment was repeated on three separate occasions to obtain a large enough number of recombinant animals.

RNAi

RNA interference was completed following the basic procedure presented by Fraser et al. (2000). RNAi was performed for all genes on LG II starting at map position 1.93 cM and moving out in both directions up to 1.78cM to the left and 2.18cM to the right.

Bacteria expressing the double stranded RNA were grown in liquid LB broth plus ampicillin. They were then placed on two RNAi plates and grown overnight. Ten L4 hermaphrodite sm*Is26[pkd-2::GFP]; rrf-3(pk1426); him-5(e1490) C. elegans* were added to one of the two plates. After 24 hours, the adult *C. elegans* were moved to the second RNAi plate. Once the eggs had hatched and reached the adult stage, fifteen males were picked from each plated and scored for CEM neurons using a fluorescent microscope. The average number of CEM neurons were recorded and used to determine if the *C. elegans* matched the *daf-19 (sm129)* phenotype.

If embryonic lethality was encountered during RNAi, the process was repeated using the *smIs26[pkd-2::GFP]; him-5(e1490)* strain rather than the *smIs26[pkd-2::GFP]; rrf-3(pk1426); him-5(e1490)* strain to reduce the effect of RNAi.

Complementation

A *daf-19(m86)* null mutant (hereafter referred to as *daf-19(-)*) was crossed with a *daf-19 (sm129)* mutant. The cross was grown at 15C. The F_1 progeny were scored for number of CEM neurons in the male. If the F_1 progeny show the mutant phenotype, it can be concluded that the

two animals have mutations in the same gene. If the F_1 progeny have the wild type phenotype, than it can be concluded that the animals have mutations in separate genes.

Sequencing

The *daf-19* locus was amplified using PCR with primers described in table1. One microliter of DNA was run on an agarose gel to determine that the proper band had been obtained and that no impurities were in the PCR product. The remaining 19 microliters of PCR product were then purified using the Bioneer Acuprep PCR purification kit (Alameda, CA).

First, a 5960 base pair segment was amplified using primers F1/R1 and worm lysate from the *smIs26[pkd-2::GFP]; daf-19 (sm129); him-5(e1490)* strain. This was sequenced using primers F1, F2, F3, F4, F5, F6, F7, F8, F9, R1, R2, and R3.

The second round of sequencing, three separate DNA fragments were isolated. The first amplified a 2220 base pair fragment using primers F17/F6 and was sequenced using primers F17, R6, F18, and F19. The second amplified a 2285 base pair fragment using primers F14/R5 and was sequenced using F14, R5, F15, and F16. The third amplified a 1159 base pair fragment using primers F11/R4 and was sequenced using primers F11, R4, F12, and F13.

A third round of sequencing only isolated a single 4403 base pair DNA fragment using primers F14/R6 and was sequenced using primer F21.

RT-PCR

RNA was extracted from both *smIs26[pkd-2::GFP]; daf-19 (sm129); him-5(e1490)* and *smIs26[pkd-2::GFP]; him-5(e1490)* strains. *C. elegans* from both strains were grown on 5 large plates each. They were washed off the plates with M9 and collected in a falcon 15 tube. The

tubes were spun and the supernatant removed. The worms were transferred to 1.5ml eppendorf tubes and spun down and the supernatant was again removed. 500 µl of Trizol was added to the tube and vortexed. The tube was then incubated at room temperature for 10 minutes. After incubating, the tube was spun at 14K for 10 minutes at 4C. The supernatant was removed to a fresh tube and to it was added 100 µl of chloroform. This was votexed for 15 seconds and left to incubate at room temperature for 3 minutes. The tube was again spun at 12K for 10 minutes at 4C. The supernatant was poured off leaving a small pellet. To the pellet was added 100µl 75% ethanol made with RNase free water. This was spun down at 7.5K for 5 minutes at 4C. The supernatant was removed and the pellet allowed to air dry. 100 µl of RNase free water was added to the pellet to dissolve the RNA. The tubes were placed on a 60C heat block for 10 minutes until the pellet went into solution. RNase free water was added to make a final concentration of 250 ng/µl. The RNA was stored at -80C. The QuantiTect Reverse Transcription Kit from Qiagen (Valencia, CA) was then used to make a cDNA library. The protocol was followed except for the following changes: step 2, 750 ng of template RNA was used and step 6, the incubation time was increased to 30 minutes.

The cDNA library was checked by PCR amplifying using *rpl-26* forward/reverse primers and then checking for bands after gel electrophoresis was completed.

The *daf-19* cDNA was then amplified using the exon 5/exon 7/8 primers. Gel electrophoresis was performed on the PCR product. The gel was 2.5% agarose and was run at 120 volts for an hour with a 50 bp ladder. The cDNA was again amplified using exon5/ exon 7/8 primers and gel electrophoresis was performed. During the second trial, the gel was 3% agarose gel run at 120 volts for 7 hours in a room at 15C. The bands were cut from the gel and purified

using the Acuprep gel purification kit. The bands were sent for sequencing using the exon 7/8 primer.

Primer sequences

Primer #	Location	Sequence
daf-19 F1	7763	gtgagttgtgaaatataattggggagtctg
daf-19 F2	8350	tgtaaatactgctctagtgc
daf-19 F3	8982	acctggatagaagtcatcc
daf-19 F4	9752	ATGTACCTACCACAGTGC
daf-19 F5	10331	TATTCAAACAACATGCAG
daf-19 F6	10983	gtggaacggaccaaacgcc
daf-19 F7	11592	GCATTGCGCTGAACATCG
daf-19 F8	12177	ACTGATGGCTACTATTGG
daf-19 F9	12814	GCGATAGTGTCATGGTGC
daf-19 F10	2367	gcgtttcgtagaacaactactatagtgc
daf-19 F11	1545	aggcacacacacatatctccttttcgtccc
daf-19 F12	2137	gatgaatgaccttcacacgg
daf-19 F13	2723	aaggctctaggtgtatgtgc
daf-19 F14	3403	ctctcagacccaaaacgaagagc
daf-19 F15	4051	tttttaaaaacaattctc
daf-19 F16	4587	gtgaaattgaaaattgag
daf-19 F17	5634	aattattgcttttctattccggctctc
daf-19 F18	6224	ataaatattcttcctacg
daf-19 F19	6783	cctataaccaccccgtct
daf-19 F20	9586	atgagaagagtgtacgaaacgcggagc
daf-19 R1	13692	ctttatgaaggcgaaaatgaaaatgaaaacc
daf-19 R2	9728	gattgtaagagaattaagctcagg
daf-19 R3	12171	CCAATAGTAGCCATCAGTGCATCC
daf-19 R4	3498	ttcccgcttttggtcacgttcacacacc
daf-19 R5	5664	aattgaaagttttttgataagccc
daf-19 R6	7827	agctcggggatgaattagcttctttgcc
22 bp *daf-19* CEM element	4014	TTCTTAATTTTTTTATAATT
daf-19 exon 5	7708	ACGATCCGAATGGCACGCGAGAGGAATTCG
daf-19 exon 7/8	10448	GCTTCCCCCGCAACGGTGAACTGGCTCTTC

Table 1: Primers and sequences used in sequencing of *daf-19 (sm129)* DNA and RNA

Results

Isolation and Initial Characterization of sm129

The *daf-19 (sm129)* mutant was recovered from an EMS screen for mutations that affect male specific neuron development of the CEM neurons (Peden et al., 2008). *daf-19 (sm129)* mutant males lack $P_{pkd\text{-}2}$*::GFP* expression in CEM head neurons (see figure 3). Wild type *C. elegans* had an average of 4 CEM neurons per animal while the *daf-19 (sm129) C. elegans* averaged 0.8 CEM neurons per animal (see table 2).

Genotype	Avg. # of CEMs per animal	
	Male	Hermaphrodite
WT	4	0
sm129	0.8	0

Table 2: scoring of male and hermaphrodite CEM neurons in wild type and *daf-19 (sm129)* animals.All strains carry *smIs26[pkd-2::GFP]* and *him-5(e1490).* CEMS were scored based on the presence/absence of GFP expression. n = 50 animals for each.

The *daf-19 (sm129)* animals also had reduced expression in the HOB and RnB tail neurons when compared to the wild type (see figure 3). $P_{pkd\text{-}2}$*::GFP* is expressed in 8 of the 9 RnB cells. *daf-19 (sm129)* mutant males lack GFP expression in R3B and have defects in R1B and R2B (see figure 3). The males were also mating deficient (data not shown). Although the CEM neurons do not express $P_{pkd\text{-}2}$*::GFP,* the *ced-3* mutation does not restore the CEM neurons showing the they are not undergoing programmed cell death but instead are not specified correctly (see table 3).

Genotype	Avg. # of CEMs per animal	
	Male	Hermaphrodite
sm129	1.4	0
ced-3(n717)	3.6	2.98
sm129; ced-3(n717)	1.3	0

Table 3: scoring of male and hermaphrodite CEM neurons in *daf-19 (sm129), ced-3(n717),* and *daf-19(sm129); ced-3(n717)* male and hermaphrodite animals showing that mutant males do not undergo programmed cell death. Strains carry *smIs23[*$P_{pkd\text{-}2}$*::GFP], dpy-10(e128),* and *him-5(e1490).* n = 50 animals for each.

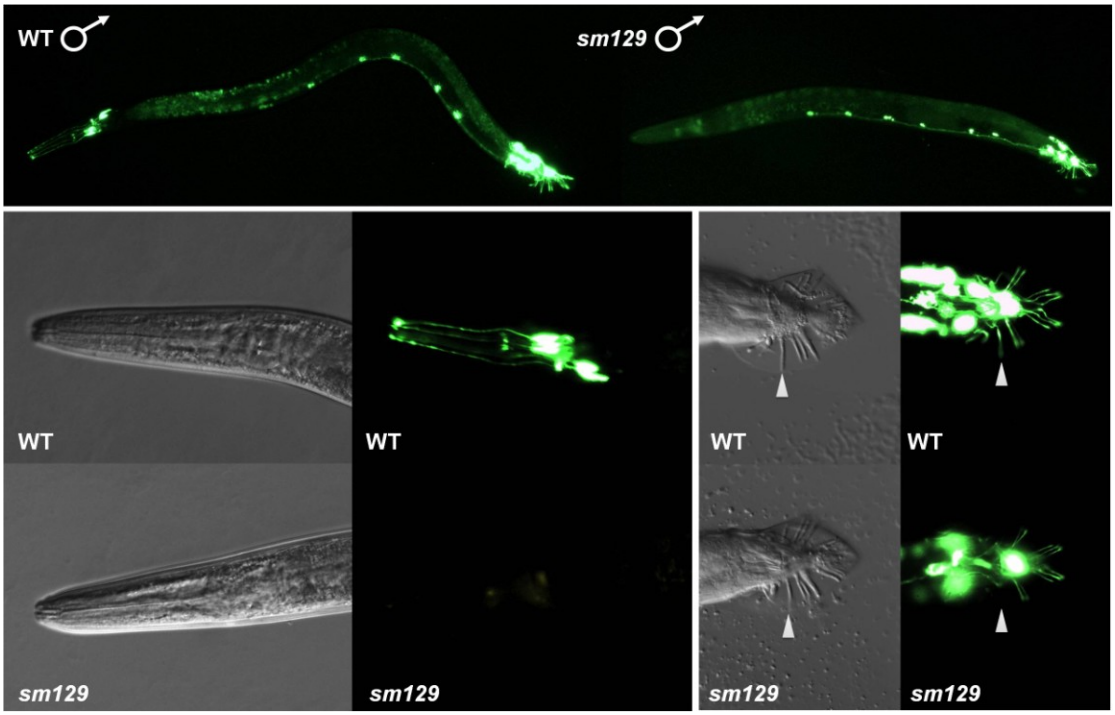

Figure 3: phenotypic expression of *daf-19(sm129).* Wild type males express four CEM head neurons in the head. *daf-19(sm129)* males completely lack expression in the CEM head neurons and have reduced expression in the HOB and RnB tail neurons as compared to wild type males. mutant males lack GFP expression in R3B and have defects in R1B and R2B

The daf-19 (sm129) mutation affects the DAF-19 transcription factor gene

daf-19 (sm129) was mapped to LG II by two-factor mapping using *dpy 10 (II:0.00 +/- 0.014 cM)* and *rol-1 (II:6.89 +/- 0.077cM)*. The position on LG II was confirmed and refined using deficiency mapping. The *daf-19 (sm129)* abnormal phenotype was observed in *daf-19 (sm129)/mnDf66*, *daf-19 (sm129)/mnDf62*, *daf-19 (sm129)/mnDf89*, and *daf-19 (sm129)/mnDf57* indicating that these four deficiencies delete the gene containing the *daf-19 (sm129)* mutation (see figure 4). The *daf-19 (sm129)* abnormal phenotype was not observed in *daf-19 (sm129)/mnDf16* or *daf-19 (sm129)/mfDf61* indicating that these two deficiencies do not delete the gene containing the *daf-19 (sm129)* mutation (see figure 4). Based on the overlapping segments of *mnDf66*, *mnDf62*, *mnDf89*, and *mnDF57* that do not overlap with *mnDf16* or *mnDf61* it was determined that the map position of *daf-19 (sm129)* was between 1.84cM and 2.83cM (see figure 4).

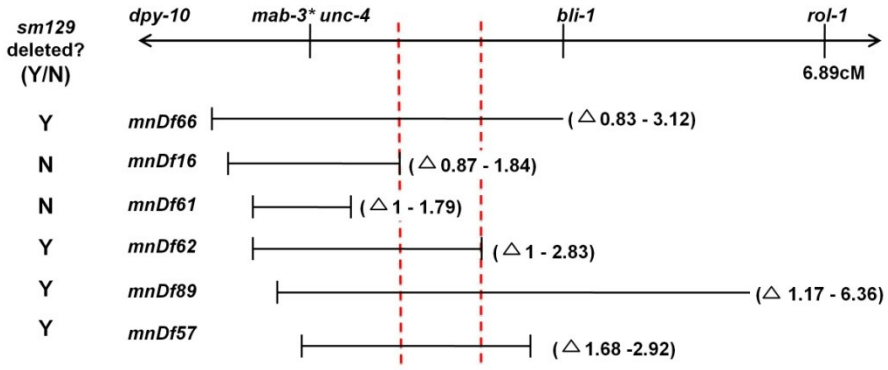

Figure 4: deficiency mapping of *daf-19(sm129)*. Based on the deficiency mapping experiment, *daf-19(sm129)* was found to be between 0.87 and 2.83 mu on chromosome II.

daf-19 (sm129)/Df showed a more severe phenotype than *daf-19 (sm129)* homozygous males. The *daf-19 (sm129)/Df* phenotype completely lacked *pkd-2::GFP* expression in the CEM head neurons and expressed less *pkd-2::GFP* in the HOB and RnB tail neurons than the *daf-19 (sm129)* homozygous males. This strongly suggests that the *daf-19 (sm129)* mutation is not a null mutation.

Based on the map position determined by deficiency mapping, a three factor mapping experiment was completed using two markers on LG II: *unc-4(e120) (II: 1.76 +/- 0.008 cM)* and *bli-1(e769) (II: 3.12 +/- 0.000 cM).* Bli non-Unc hermaphrodites were collected and scored for the *daf-19 (sm129)* phenotype. This experiment was completed on three separate occasions. During the first trial, 7/7 of the *bli-1(e769) non-unc-4(e120)* hermaphrodites expressed the *daf-19 (sm129)* phenotype. During the second trial 10/12 of the *bli-1(e769) non-unc-4(e120)* hermaphrodites expressed the *daf-19 (sm129)* phenotype. During the third trial 13/15 of the *bli-1(e769) non-unc-4(e120)* hermaphrodites expressed the *daf-19 (sm129)* phenotype. Using all three trials, 30/34 of the *bli-1(e769) non-unc-4(e120)* hermaphrodites expressed the *daf-19 (sm129)* phenotype which placed the *daf-19 (sm129)* map position at 1.93cM. Three-factor mapping was also done collecting *unc-4(e120) non-bli-1(e769)* hermaphrodites. This was completed in two separate trials. During the first trial, 0/5 of the *unc-4(e120) non-bli-1(e769)*

hermaphrodites expressed the *daf-19 (sm129)* phenotype. During the second trial, 0/2 of the *unc-4(e120) non-bli-1(e769)* hermaphrodites expressed the *daf-19 (sm129)* phenotype. Because no *unc-4(e120) non-bli-1(e769)* hermaphrodites were isolated that expressed the *daf-19 (sm129)* phenotype, these experiments were not useful in the determination of the map position of *daf-19 (sm129).*

A RNAi screen for candidate genes in the area that *daf-19 (sm129)* mapped to was conducted (see Materials and Methods). RNAi treatment against *daf-19,* located at map position 2.16cM was the only RNAi treatment that phenocopied *daf-19 (sm129)*. Males from *daf-19(RNAi)* were observed for expression of *pkd-2::GFP* in the CEM head neurons. The males showed reduced expression of *pkd-2::GFP* averaging 2.7 CEM neurons per animal (compared to an average of 4 CEM neurons per animal in wild type males) (see table 4).

A complementation test was performed by crossing *smIs26[pkd-2::GFP]; daf-19 (sm129)/mIn1(mIs14); him-5(e1490)* males with *smIs26[pkd-2::GFP]; daf-19 (-)* hermaphrodites at 15C. The F_1 males were observed for expression of *pkd-2::GFP* in the CEM head neurons. Of the thirteen males observed, an average of zero CEM neurons per animal were present (compared to an average of 4 CEM neurons per wild type male). *daf-19(null)* males were also examined and of the two animals inspected had an average of zero CEM neurons were present (see table 4).

Genotype	Avg. # of CEMs per animal (*n*)
Wild Type (control RNAi)	4 (50)
daf-19(RNAi)	2.7 (30)
sm129	0.8 (50)
daf-19(null)	0 (2)
daf-19(null)/sm129	0 (13)

Table 4: number of CEM neurons in the head of male wild type, *daf-19(RNAi), daf-19(sm129), daf-19 null (m86),* and *daf-19 null (m86)/daf-19(sm129) C. elegan.* The number of animal observed in each is show in parentheses next to the average number of CEM neurons.

The daf-19 (sm129) mutation is a point mutation at the 3' end of the intron before exon 6

Since mapping data, RNAi phenocopy, and non-complementation all suggested that the *daf-19(sm129)* mutation is an allele of *daf-19*, the *daf-19* locus was sequenced from *daf-19(sm129)* mutant animals (see Materials and Methods). The obtained sequence was compared

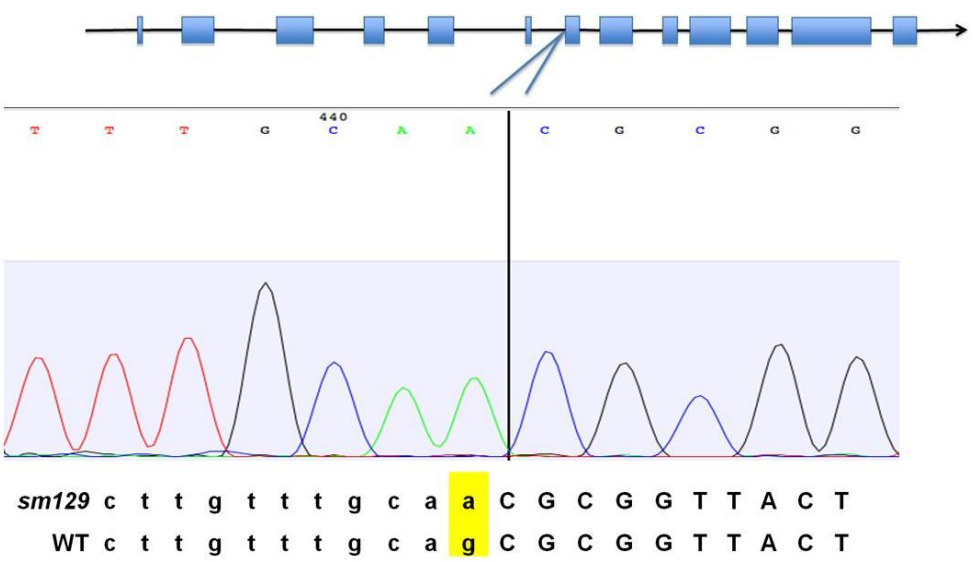

Figure 5: *daf-19(sm129)* sequence data compared with wild type sequence data at the 3' acceptor site of exon 6. There is a point mutation from ag (in wild type) to aa (in *daf-19(sm129)*).

to the wild type sequence of *daf-19* presented in WormBase. A single point mutation was discovered at the 3' end of the intron before exon 6 changing the cag consensus sequence to caa (figure 5). Although *C.* elegans introns always end in caa, Aroian et al. (1993) showed that a point mutation of cag to caa at the 3' splice acceptor site does not always prevent proper splicing; the mutation leads to a portion of correct splicing as well as splicing to a nearby ag either up or downstream from the splice acceptor site. No other mutations were discovered in sequencing the entire *daf-19* locus from the 5' regulatory sequences past the stop codon.

daf-19 (sm129) mRNA of daf-19 splices correctly a portion of the time

RT-PCR was used to determine if proper splicing of exon 6 occurred. Using the exon 5 forward primer and the exon 7/8 reverse primer, we expected to see a band at 269 base pairs if proper splicing occurred. We expected a band at 299 base pairs (in frame) if splicing occurred at

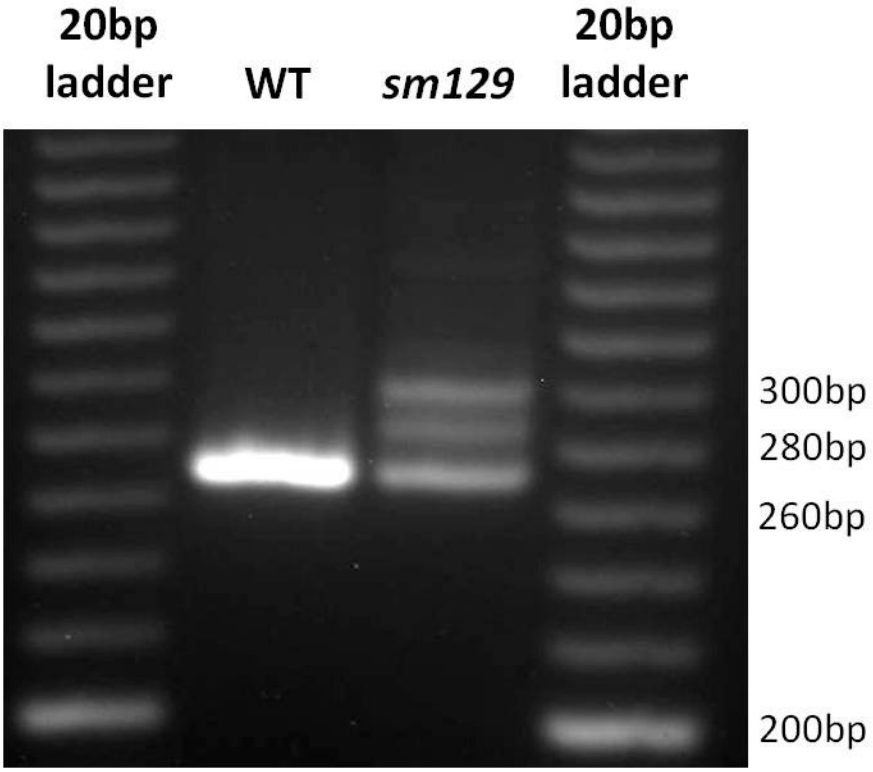

Figure 6: gel electrophoresis of wild type and *daf-19(sm129)* RNA amplified using RT-PCR with the exon 5 primer and the exon 7/8 primer. The wild type had one band at the expected length of 269 base pairs if proper splicing occurred. The *daf-19(sm129)* had three bands: one at the expected length of 269 base pairs if proper splicing occurred, one around 280 base pairs that did not sequence cleanly and therefore it is unknown where splicing occurs, and one at 299 that showed splicing had occurred at the next upstream ag and caused no frame shift.

the next upstream ag and a band at 202 base pairs (out of frame) if exon 6 was skipped completely. A single band at 269 base pairs was observed in the wild type animals while three separate bands appeared at 269, 280, and 299 base pairs in the *daf-19 (sm129)* animals (figure 6). All four bands were cut out of the bands and sequenced. The sequence of the wild type band showed proper splicing had occurred. In the *daf-19 (sm129)* animals, the sequence of the lowest

band (at 269 base pairs) also showed proper splicing. The sequence of the middle band at 280 base pairs did not sequence cleanly. The sequence of the top band at 299 base pairs showed splicing had occurred at the next upstream ag and that no frame shift had occurred.

The daf-19 (sm129) mutation does not affect IFT

A *daf-19 (sm129); osm-6; him-5(e1490) C. elegans* strain was produced and compared to a *osm-6; him-5(e1490) C. elegans* strain. Neurons were observed and counted in both males and hermaphrodites. No differences were observed between male and hermaphrodite *daf-19 (sm129)* and wild type animals when observed with fluorescence microscopy (figure 7).

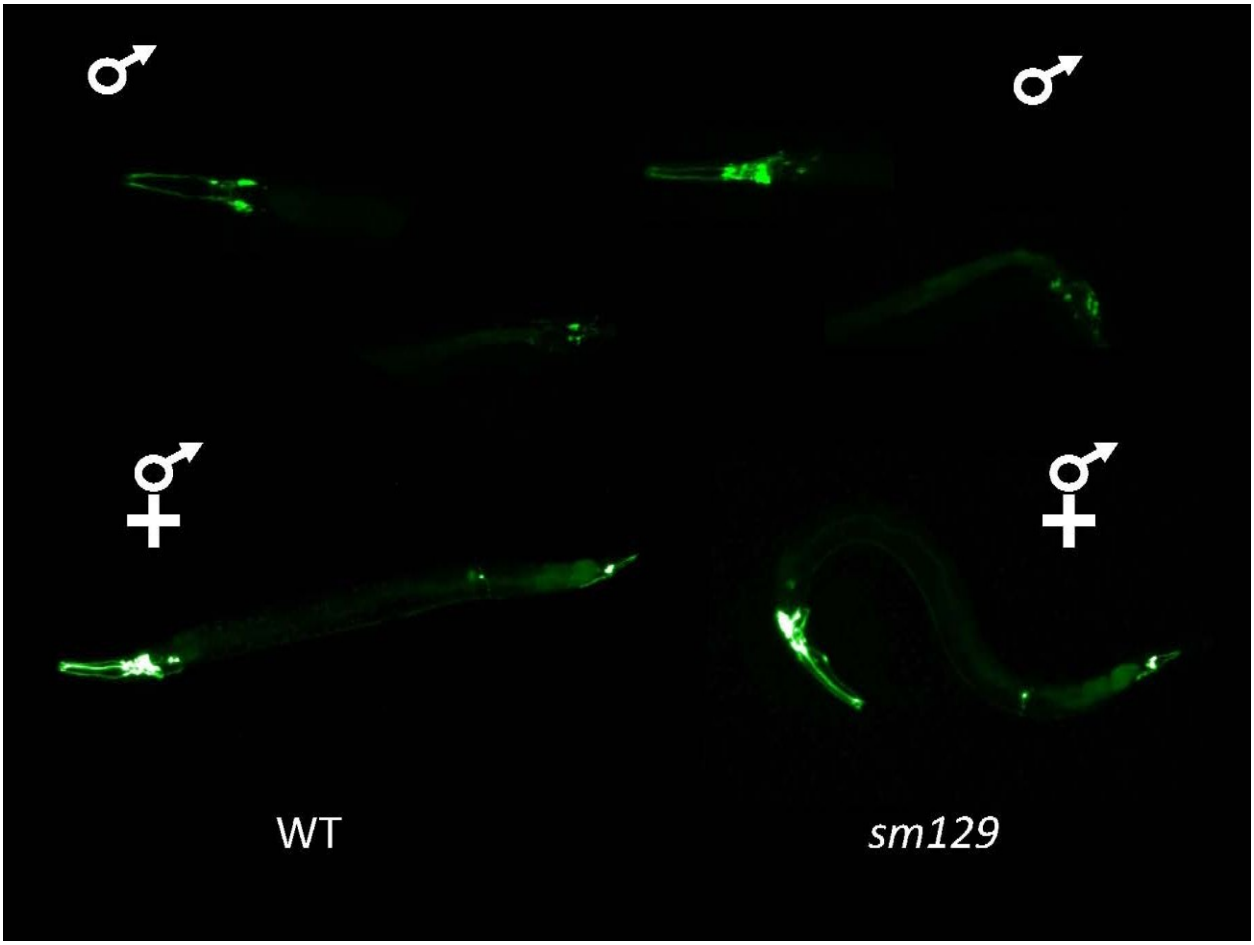

Figure 7: *osm-6; him-5(e1490)* and *daf-19(sm129); osm-6; him-5(e1490)* males (top) and hermaphrodites (bottom) shown with the *OSM-6::GFP* marker. No differences were observed between wild type and *daf-19(sm129)* hermaphrodites

Discussion

The *sm129* mutation inhibits expression of the CEM head neurons in male *C. elegans* and reduces expression in the RnB and HOB tail neurons. The *sm129* mutation mapped to the *daf-19* gene at the 3' AG splice acceptor site before exon 6 and interrupts correct splicing of exon 6 a portion of the time. Because incorrect splicing only occurs a portion of the time, the mutation is less severe than either the *daf-19(-)*allele or the *daf-19(n4132)* allele that has a mutation in a regulatory element.

The *daf-19(-)*animals express the dauer phenotype (Swoboda et al., 2000) while the *daf-19 (sm129)* mutant does not express this phenotype. The *daf-19(-)* mutant lacks all sensory cilia as evidenced by loss of *osm-6::*GFP expression and completely lacks expression of $P_{pkd\text{-}2}$*::GFP* in the CEM head neurons and the RnB and HOB tail neurons (Swoboda et al., 2000 and Yu et al., 2003). The *daf-19 (sm129)* mutant does not lack all sensory cilia and does not lack *osm-6::GFP* expression, but it does lack expression of $P_{pkd\text{-}2}$*::GFP* expression in the PKD and HOB neurons showing that the *daf-19 (sm129)* mutation only affects specification of sensory neurons. Thus we can conclude that *sm129* is a reduction of function allele and affects only a subset of the phenotypes that the null allele affects.

The *daf-19 (n4132)* is less severe. Like *daf-19 (-)* and *daf-19 (sm129)* mutants, *daf-19 (n4132)* mutants lack expression of $P_{pkd\text{-}2}$*::GFP* in the CEM head neurons (Wang et al., 2010). Although both *daf-19 (sm129)* and *daf-19 (n4132)* mutants lack $P_{pkd\text{-}2}$*::GFP* in the CEM head neurons, the *daf-19 (n4132)* mutants completely lack $P_{pkd\text{-}2}$*::GFP* in the RnB and HOB tail neurons while the *daf-19 (sm129)* mutants only have reduced $P_{pkd\text{-}2}$*::GFP* in the RnB and HOB neurons (Wang et al., 2010). Similar to *daf-19 (sm129)*, *daf-19 (n4132)* mutants do not affect expression of *osm-6::GFP* (Wang et al., 2010).

Because the *daf-19 (-)* mutant expresses the dauer phenotype and also prevents proper differentiation and specification of ciliated neurons while the *daf-19 (sm129)* and *daf-19 (n4132)* only affect different levels of specification we predict that different levels of properly spliced *daf-19* mRNA are required to control each phenotype. As shown by the RT-PCR gel electrophoresis and sequencing of both wild type and *daf-19 (sm129)* mRNA, *daf-19* is spliced correctly a portion of the time. We predict that these decreased levels of properly spliced *daf-19* mRNA are sufficient to prevent dauer formation and cause proper differentiation of ciliated neurons but the mRNA are not sufficient to cause proper specification of the ciliated neurons. We predict that the lowest level of mRNA will prevent dauer formation while intermediate levels of mRNA will cause proper differentiation of ciliated neurons and the highest levels of mRNA are required for proper specification of mRNA.

In the future, we will use quantitative RT-PCR (qRT-PCR) to determine the percentage of mRNA that is being spliced correctly in the *daf-19 (sm129)* mutant. This information will be used to determine a better estimate on the amounts of *daf-19* mRNA that is required to prevent expression of the dauer phenotype as well as cause proper differentiation of ciliated neurons without proper specification of these neurons. Along with using qRT-PCR to determine mRNA levels, we also will use a transgenic cDNA to attempt to rescue the mutant phenotype.

References

Aftab, Syed, Lucie Semenec, Jeffrey Shih-Chieh Chu and Nansheng Chen. 2008. Identification and characterization of novel human tissue-specific RFX transcription factors. *BMC evolutionary biology*. **8:** 226-237.

Aroian, Raffi V, Adam D. Levy, Makoto Koga, Yasumi Ohshima, James M. Kramer, and Paul W. Sternberg. 1993. Splicing in *Caenorhabditis elegans* does not require an AG at the 3' splice acceptor site. *Molecular and cellular biology.* **13:** 626-637.

Bae, Young-Kyung and Maureen M. Barr. 2008. Sensory roles of neuronal cilia: cilia development, morphogenesis, and function in *C. elegans*. *Frong Biocsi*. **13:** 5959-5974.

Barr, Maureen M, John DeModena, Douglas Braun, Can Q. Nguyen, David H. Hall, and Paul W. Steinberg. 2001. The *Caenorhabditis elegans* autosomal dominant polycystic kidney disease gene homologs *lov-1* and *pkd-2* act in the same pathway. *Current biology*. **11:** 1341-1346.

Barr, Maureen M. and Paul W. Sternberg. A polycystic kidney-disease gene homologue required for male mating behavior in *C. elegans*. *Nature*. **401:** 386-389.

Bonnafe, E, M. Touka, A. AitLounis, D. Baas, E. Barras, C. Ucla, A. Moreau, F. Flamant, R. Dubruille, P. Couble, J. Collignon, B. Durand, and W. Reith. 2004. The transcription factor RFX3 directs nodal cilium development and left-right asymmetry specification. *Molecular and cellular biology*. **24:** 4417-4427.

Burghoorn, Jan, Brian P. Piasecki, Filip Crona, Prasad Phirke, Kristian E. Jeppsson, and Peter Swoboda. 2012. The in vivo dissection of direct RFX-target gene promoters in *C. elegans* reveals a novel *cis*-regulatory element, the C-box. *Developmental biology*. **368:** 415-426.

Cavalier-Smith, T. 2002. The phagotrophic origin of eukaryotes and phylogenetic classification of Protozoa. *International Journal of Systematic and Evolutionary Microbiology.* **52:** 297-354.

Chasnov, J. R, W. K. So, C. M. Chan, and K. L. Chow. 2007. The species, sex, and stage specificity of a *Caenorhabditis* sex pheromone. *Proceedings of the national academy of sciences of the United States of America*. **104:** 6730-6735.

Chung, Mei-I, Sara M. Peyrot, Sarah LeBoeuf, Tae Joo Park, Kriston L. McGary, Edward M. Marcotte, and John B. Wallingford. 2012. RFX2 is broadly required for ciliogenesis during vertebrate development. *Developmental biology*. **363:** 155-165.

Emery, Patrick, Bénédicte Durand, Bernard Mach, and Walter Reith. 1996. RFX proteins, a novel family of DNA binding proteins conserved in the eukaryotic kingdom. *Nucleic acids research*. **24:** 803-807.

Fliegauf, Manfred, Thomas Benzing, and Heymut Omran. 2007. When cilia go bad: cilia defects and ciliopathies. *Nature reviews molecular cell biology.***8:** 880-893.

Fraser, Andrew G, Ravi S. Kamath, Peder Zipperlen, Maruxa Martinez-Campos, Marc Sohrmann, and Julie Ahringer. 2000. Functional genomic analysis of *C. elegans* chromosome I by systematic RNA interference. *Nature*. **408:** 325-330.

Hartwell, Leland H., Leroy Hood, Michael L. Goldberg, Ann E. Reynolds, Lee M. Silver, Ruth C. Veres. 2008. Reference C *Caenorhabditis elegans*: genetic portrait of a simple multicellular animal. *Genetics From Genes to genomes*. Third edition. McGraw-Hill.

Hirokawa, Nobutaka. 1998. Kinesin and dynein superfamily proteins and the mechanism of organelle transport. *Science.* **279:** 519-526.

Ibañez-Tallon, Inés, Nathaniel Heintz, and Heymut Omran. 2003. To beat or not to beat: roles of cilia in development and disease. *Human molecular genetics.* **12:** 27-35.

Inglis, Peter N, Keith A. Boroevich, and Michel R. Leroux. 2006. Piecing together a ciliome. *Trends in Genetics*. **22:** 491-500.

Liu, Katharine S. and Paul W. Sternberg. 1995. Sensory regulation of male mating behavior in *Caenorhabditis elegans*. *Neuron*. **14:** 79-89.

Peden, Erik M. and Maureen M. Barr. 2005. The KLP-6 kinesin is required for male mating behaviors and polycystin localization in *Caenorhabditis elegans*. *Current biology*. **15:** 394-404.

Peden, Erin, Darrell J. Killian, and Ding Xue. 2008. Cell death specification in *C. elegans*. *Cell cycle*. **7:** 2479-2484.

Reiter, Jeremy F. 2008. A cilium is not a cilium is not a cilium: signaling contributes to ciliary morphological diversity. *Developmental Cell*. **14:** 635-636.

Reith, Walter, Carlos Herrero-Sanchez, Michel Kobr, Paolo Silacci, Christine Berte, Emanuelle Barras, Sylvia Fey, and Bernard Mach. 1990. MHC class II regulatory factor RFX has a novel DNA-binding domain and a functionally independent dimerization domain. *Genes and development.* **4:** 1528-1540.

Reith, W, C. Ucla, E. Barras, A. Gaud, B. Durand, C. Herrero-Sanchez, M. Kobr, and B. Mach. 1994. RFX1, a transactivator of hepatitis B virus enhancer I, belongs to a novel family of homodimeric and heterodimeric DNA-binding proteins. *Molecular and cellular biology.* **14:** 1230-1244.

Rosenbaum, Joel L. and George B. Witman. 2002. Intraflagellar transport. *Molecular cell biology*. **3:** 813-825.

Satir, Peter, Søren T. Christensen. 2008. Structure and function of mammalian cilia. *Histochem Cell Biology*. **129:** 687-693.

Senti, Gabriel and Peter Swoboda. 2008. Distinct isoforms of the RFX transcription factor DAF-19 regulate ciliogenesis and maintenance of synaptic activity. *Molecular biology of the cell*. **19:** 5517-5528.

Simon, Jasper M. and Paul W. Sternberg. 2002. Evidence of a mate-finding cue in the hermaphrodite nematode *Caenorhabditis elegans*. *PNAS*. **99:** 1598-1603.

Singla, Veena and Jeremy F. Reiter. 2006. The primary cilium as the cell's antenna: signaling at a sensory organelle. *Science*. **313**: 629-633.

Snow, Joshua J, Guangshuo Ou, Amy L. Gunnarson, M. Regina S. Walker, H. Mimi Zhou, Ingrid Brust-Mascher, and Jonathan M. Scholey. 2004. Two anterograde intraflagellar transport motors cooperate to build sensory cilia on *C. elegans* neurons. *Nature cell biology*. **6:** 1109-1113.

Swoboda, Peter, Haskell T. Adler, and James H. Thomas. 2000. The RFX-type transcription factor DAF-19 regulates sensory neuron cilium formation in *C. elegans*. *Molecular cell*. **5:** 411-421.

Tuch, Brian B, Hao Li, and Alexander D. Johnson. 2008. Evolution of eukaryotic transcription circuits. *Science*. **319:** 1797-1799.

Wang, Juan, Hillel T. Schwartz, and Maureen M. Barr. 2010. Functional specialization of sensory cilia by an RFX transcription factor isoform. *Genetics.* **186:** 1295-1307.

Yu, Hui, René F. Prétôt, Thomas R. Bürglin, and Paul W. Sternberg. 2003. Distinct roles of transcription factors EGL-46 and DAF-19 in specifying the functionality of a polycystin-expressing sensory neuron necessary for *C. elegans* male vulva location behavior. *Development*. **130:** 5217-5227.